Open Research Online

The Open University's repository of research publications
and other research outputs

Evolution of proton-induced defects in a cryogenically irradiated p-channel CCD

Conference or Workshop Item

How to cite:

Wood, Daniel; Hall, David; Gow, Jason; Murray, Neil; Stefanov, Konstantin and Holland, Andrew (2017). Evolution of proton-induced defects in a cryogenically irradiated p-channel CCD. In: 2016 16th European Conference on Radiation and Its Effects on Components and Systems (RADECS), IEEE, Piscataway, NJ.

For guidance on citations see FAQs.

© 2016 by the Institute of Electrical and Electronics Engineers

Version: Version of Record

Link(s) to article on publisher's website:
http://dx.doi.org/doi:10.1109/RADECS.2016.8093129
http://ieeexplore.ieee.org/document/8093129/

Copyright and Moral Rights for the articles on this site are retained by the individual authors and/or other copyright owners. For more information on Open Research Online's data policy on reuse of materials please consult the policies page.

oro.open.ac.uk

Evolution of proton-induced defects in a cryogenically irradiated p-channel CCD

Daniel Wood, David J. Hall, Jason Gow, Neil J. Murray, Konstantin Stefanov, Andrew D. Holland

***Abstract*—P-channel CCDs have been shown to display improved tolerance to radiation-induced charge transfer inefficiency (CTI) when compared to n-channel CCDs. This is attributed to the properties of the dominant charge-trapping defect species in p-channel silicon relative to the operating conditions of the CCD. However, precise knowledge of defect parameters is required in order to correct for any induced CTI. The method of single trap-pumping allows us to analyse the defect parameters to a degree of accuracy that cannot be achieved with other common defect analysis techniques such as deep-level transient spectroscopy (DLTS). We have analysed using this method the defect distribution in an e2v p-channel CCD204 irradiated with protons at cryogenic temperature (153K). The dominant charge trapping defects at these conditions have been identified as the donor level of the silicon divacancy and the carbon interstitial defect. The defect parameters are analysed both immediately post irradiation and following several subsequent room-temperature anneal phases. The evolution of the defect distribution over time and through each anneal phase provides insight into defect interactions and mobility post-irradiation. The results demonstrate the importance of cryogenic irradiation and annealing studies, with large variations seen in the defect distribution when compared to a device irradiated at room-temperature, which is the current standard procedure for radiation testing.**

***Index Terms*—Divacancy, CCD, p-channel, defect, pocket pumping, radiation damage, Carbon, trap pumping**

I. Introduction

Radiation-induced defects are responsible for charge-transfer performance degradation in CCDs because they introduce stable deep-levels within the silicon band-gap, which are capable of trapping a single charge carrier (h^+ for the p-channel case) for a length of time before emitting it again [1]. This finite time is heavily temperature dependent and is defined as the defect emission time-constant (τ_e). Where the emission time-constant at a given temperature is close to the line transfer time of the CCD, charge carriers can be moved efficiently between adjacent charge-packets, leading to image smearing [2] which is detrimental to the science goals of the detector [3].

P-channel CCDs have demonstrated improved tolerance to radiation damage induced image degradation because the predominant defects produced; the donor level of the silicon divacancy and the carbon interstitial defect, both have emission time-constants which interfere less with the typical CCD operating conditions at nominal space-based detector temperatures than in the n-channel case [4].

However, previous studies have also shown considerable uncertainty in defect emission time-constants, of up to an order of magnitude [5]. It is therefore vital both for a complete comparison between n- and p-channel CCDs and for future mitigation of radiation-induced CTI to study with high precision the parameters of defects produced in p-type silicon post-irradiation.

D. Wood, D. J. Hall, J. Gow, K. Stefanov and A. Holland are with the *Centre for Electronic Imaging*, Department of Physical Sciences, The Open University, Milton Keynes, MK76AA, UK. (email: daniel.wood@open.ac.uk; david.hall@open.ac.uk; konstantin.stefanov@open.ac.uk; jason.gow@open.ac.uk; andrew.holland@open.ac.uk). N. J. Murray is with Dynamic Imaging Analytics Limited, Bletchley Park Science and Innovation Centre, Sherwood Drive, Bletchley, MK3 6EB. (email: neil.murray@dynamicimaginganalytics.co.uk)

II. Trap pumping

The charge trapping process is described by Shockley-Read-Hall kinetics [6][7] which models the capture and release of electrons (or holes) through the use of two exponential time constants; the capture time-constant and emission time-constant, as shown in Equations 1 and 2. Here σ is the cross-section, n is the electron concentration, E is the energy of the level above the valence band edge and m^* is the effective hole mass.

$$\tau_c = \frac{1}{\sigma n v_{th}} \tag{1}$$

$$\tau_e = \frac{1}{\sigma N_v v_{th}} \exp\left(\frac{E}{kT}\right) \tag{2}$$

$$N_v = 2\left(\frac{2\pi m^* kT}{h^2}\right)^{\frac{3}{2}} \tag{3}$$

$$v_{th} = \sqrt{\frac{3kT}{m^*}} \tag{4}$$

As previously stated the emission time-constant is the defect parameter which governs how destructive the defect can be to charge transfer performance. At the signal levels used throughout this study it is acceptable to assume instant capture, i.e $\tau_e >> \tau_c$ [8] .

To analyse the defect emission time-constants the method of trap pumping is used, which is described fully in [8] and [9]. Trap pumping allows for direct analysis of the defect time constants by running the CCD in such a way as to amplify the effects of any relevant charge-trapping defects. This is achieved by "shuffling" charge back and forth between two adjacent pixels many times, before reading out the CCD conventionally. Each time charge is shuffled from one pixel to the next and back there exists a probability that a defect will capture a charge carrier from one charge packet and release it at a later time into an adjacent packet. Over many cycles

978-1-5090-4366-8/16/$31.00 ©2016 IEEE

this leads to characteristic dipoles within the final image, the intensity of which depends on the "dwell time" between each shuffle of charge, and the emission time-constant of the responsible defect. Monitoring the efficiency of a defect to effectively trap charge with respect to this dwell time allows for calculation of τ_e as shown in [8].

A major advantage of this technique is that each defect can be studied on an individual basis, which is in contrast to other defect analysis methods such as DLTS which rely on the combined effects of many defects [10].

III. Cryogenic Irradiation

Using the trap pumping method we have analysed the defects produced in a p-channel CCD204 following irradiation with protons at cryogenic temperature (153K). Results from a room-temperature proton irradiation of a CCD204 were used for comparison and to identify the most probable defect distribution post-irradiation. Under the conditions of this study two defect species dominate charge-transfer degradation; a donor level of the silicon divacancy (VV(+/0)) and the carbon interstitial defect (Ci) [5].

Measurements were performed at 153k post-irradiation and then subsequently after periods of 1-day, 1-week and 1-month annealing at room temperature.

The e2v CCD204 is a 4k x 1k device which utilises a split output register with two separate output nodes. For this study two CCD204 devices were irradiated at the Synergy Health 5MV Tandem Accelerator (UK) [11].

One device was held at room temperature during irradiation and received a 10MeV equivalent proton fluence of 2×10^9 pcm^{-2}. A second device was held at cryogenic temperature (153K) and received a 10MeV equivalent fluence of 1.24×10^9 pcm^{-2}. The irradiated regions were chosen such as to leave the output nodes unirradiated. Full details of the irradiation are outlined in [11].

A cryogenic irradiation was performed in order to more closely mirror the conditions in a typical space-based detector as impinging particles strike the CCD. The room temperature irradiation allowed for an instant comparison and gave a start point for the expected defect distribution in the cryogenically irradiated device.

Defect emission time-constant distributions immediately post-irradiation for the room-temperature device are shown in Figure 1(a). The room-temperature results have been scaled to reflect the higher fluence received by this device, by assuming a linear relationship between fluence and the number of defects produced. Initial results from the room-temperature device showed the donor level of the divacancy to be by far the most abundant defect produced, with a dominant peak in the emission time constant distribution at 30 µs. Slower defects are also present but there is no clear second peak in the distribution corresponding to another defect species.

Initial results from the cryogenic device are shown in Figure 1(b) and show far fewer defects produced than in the room-temperature case. Although a small peak in the emission time constant distribution is present at typical divacancy range there is no clearly identifiable defect species present in large numbers.

Following analysis of the initial distributions a trap pumping method with reduced temporal resolution was used on the cryogenic device to study defect evolution in the first few hours after irradiation. The defect distribution was re-analysed every few hours over a period of several days until the first room-temperature anneal stage, with the number of (probable) divacancy defects tracked over time. The results are shown in Figure 2(a).

For the first few days after irradiation there are small variations in the number of defects found, showing that the situation is still dynamic. This is shown more clearly in Figure 2(b) which is simply a zoomed in image of Figure 2(a). Defects may be mobile or able to disassociate/recombine even at cryogenic temperatures. Changes are still visible right up until the point of the first anneal stage, at around 120 hours after irradiation. The device was annealed for 1-day at room-temperature before being cooled back down to 153K for testing. Immediately obvious is the large increase in the number of divacancy defects found after anneal, with the defect distribution more closely resembling the room-temperature device at this stage.

IV. Annealing

A full trap-pumping analysis of the cryogenic device was carried out after the 1-day anneal stage, producing the defect emission time-constant distribution for several temperatures within the range 143K-173K . The temperature dependence of the emission time constant (see Equation 2) allows for a calculation of both the defect energy level within the band-gap and the cross-section.

Further anneal stages were carried out resulting in a total anneal time of 1-week and 1-month. A major advantage of trap pumping is the ability to identify individual defects which are present after each anneal stage and to monitor their emission time constants, energy levels and capture cross-sections on an individual basis [8]. The large number of defects present gives good statistics and therefore a highly accurate calculation of defect parameters.

Emission time constant distributions for all fitted defects at 153K following each anneal stage are shown in Figure 1(c), Figure 1(d) and Figure 1(e). Each shows a large peak around the expected divacancy emission time constant; however the situation is dynamic, with the divacancy distributions non-Gaussian and containing two or more discernible peaks. From these distributions it appears as though many of the defects are moving and/or re-orienting over these time scales, and that the overall defect distribution is tending towards the room-temperature case, i.e. divacancy dominated.

Energy levels and cross-sections were calculated at each anneal stage for all defects which appear at every temperature. Figure 3 shows the resulting energy distribution for the 1-day anneal stage. We find for the large peak an energy level and capture cross-section of $E_v + 0.19(\pm 0.01)$ eV and $10^{-15.5\pm0.5}$ cm^2 respectively which are consistent with the values of $E_v + 0.19$ eV and $10^{-15\pm0.3}$ cm^2 found by Mostek *et al.* [5] for the divacancy donor level.

The smaller peak contains much fewer defects but shows a Gaussian energy distribution. We find for this peak an energy

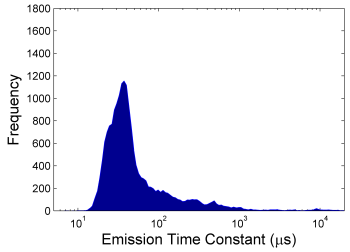

(a) Room-temperature irradiated device. The results have been normalised to the fluence recieved by the cryo device.

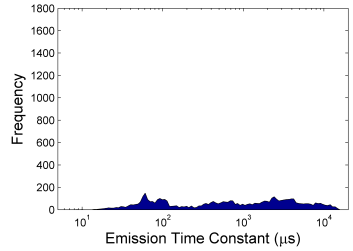

(b) Cryogenically irradiated device, immediately post-irradiation.

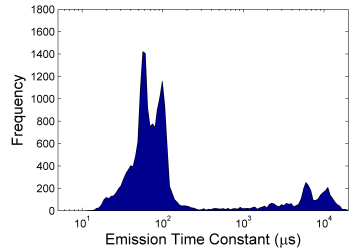

(c) Cryo device following 1-day anneal.

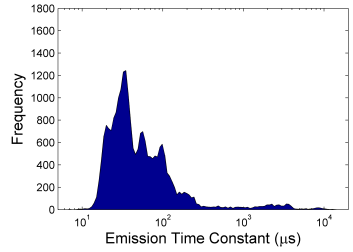

(d) Cryo device following 1-week anneal.

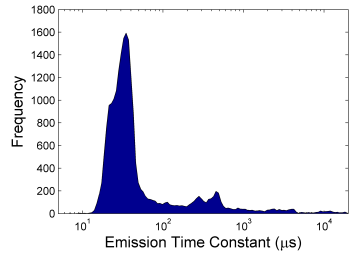

(e) Cryo device following 1-month anneal.

Fig. 1: Defect emission time-constant distributions for both devices at various stages throughout the study. Each anneal stage was performed at room-temperature.

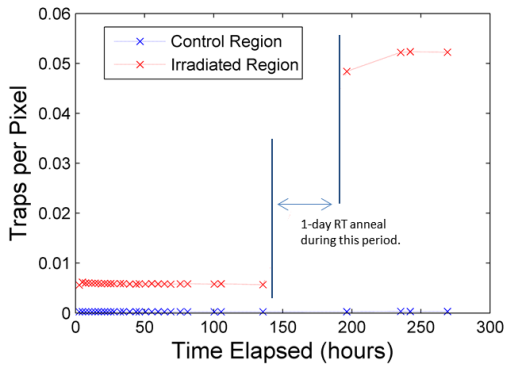

(a) Divacancy defects per pixel against time elapsed since irradiation, for the cryogenically irradiated device. Includes the 1-day anneal stage as specified. The connecting lines are drawn only for clarity.

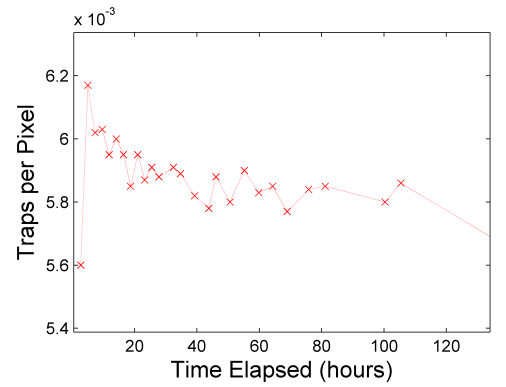

(b) A zoomed in image of the first 120 hours after irradiation, showing that there are small variations whilst the device remains cold.

Fig. 2: Divacancy defects per pixel found in the cryogenically irradiated device post-irradiation using the trap-sweeping method. The connecting lines are drawn only for clarity.

level and capture cross-section of $E_v + 0.27(\pm 0.01)$ eV and $10^{-13.8\pm0.4}$ cm^2 respectively which is also consistent with the values of $E_v + 0.28$ eV and $10^{-14.5\pm0.4}$ cm^2 found by Mostek *et al.* for the carbon interstitial level [5]. It should be noted however that previous studies have considered the overall effects of many defects, where as the values quoted in this study come from the distributions of individually analysed defects, on which the measurement uncertainty is negligible compared to the width of the overall distribution.

Both the donor level of the divacancy and the carbon interstitial were found to be present after each anneal stage, with no variation in calculated energy-level or cross-section within the observed spread. The energy distributions are strongly Gaussian, which implies no other stable defect species are involved that can be detected. Therefore the separate time-constant peaks seen for both the divacancy and the carbon interstitial most probably relate to different orientations of the same defect. It is clear from the defect densities, locations and time-constants that there are large changes occurring in the defect distributions over these time scales at room-temperature.

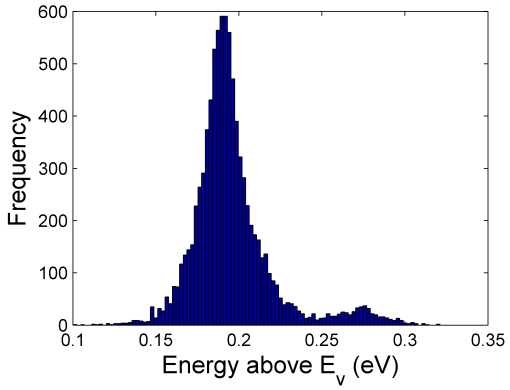

Fig. 3: Energy distribution for all fitted defects found at 143K, 153K and 163K after the 1-day room-temperature anneal stage. The distribution of energies originates from calculating the energy level of each individual defect based on time-constant measurements, for which the measurement uncertainty is small (approximately 5%). This uncertainty is negligible compared to the width of the distribution.

V. Conclusions

Using the method of trap pumping we have studied radiation induced defects in a p-channel CCD irradiated with protons at 153K. The defect emission time constants have been calculated at various time intervals both immediately following irradiation and after subsequent anneal phases of 1-day, 1-week and 1-month.

Calculation of the defect energy levels and capture-cross-sections show that the dominant charge capturing defect under our operating conditions is the donor level of the silicon divacancy, with a calculated energy level of $E_v + 0.19(\pm 0.01)$ eV. Also present is a carbon interstitial defect with an energy $E_v + 0.27(\pm 0.01)$ eV.

Whilst the energy distributions show two dominant defect species appearing at all stages, the emission time-constant distributions as well as the defect densities and locations show dynamic changes over these time scales. In particular more than one peak is observed in both the divacancy and carbon interstitial time-constant distributions at various times. Further investigation is therefore required in this area.

The importance of cryogenic irradiation and annealing studies as opposed to the more standard technique of irradiating at room-temperature is apparent both because of the large differences in initial defect distributions and because of the major changes taking place during each anneal stage. It is also evident that if a cryogenic irradiation results in a more preferable defect distribution than for the room-temperature case, then the device must be kept cold in order to maintain this distribution. Precise knowledge of defect parameters is vital in order to mitigate for radiation-induced CTI and so further analysis in this area provides scope for improved radiation tolerance of space-based detectors.

Throughout this study we have considered only p-channel devices, and hence only hole traps. In n-channel devices, which remain the current standard for space-based detectors, similar studies into the effects of a cryogenic irradiation on the electron trap distribution are ongoing [12][13][14].

Acknowledgements

The authors would like to thank Keith Jones of Synergy Health for his assistance during the proton irradiation, and Ludovic Duvet, Thibaut Prodhomme and Alessandra Ciapponi of ESA for their support during the early stages of this study. With thanks also to e2v for providing the devices used throughout this study.

References

[1] G. Watkins, "Intrinsic defects in silicon," *Materials Sci. in semiconductor processing*, pp.227-235, 2000.

[2] R. Massey, C. Stoughton, A. Leauthaud, J. Rhodes, A. Koekemoer, R. Ellis and E. Shaghoulian,"Pixel-based correction for charge transfer inefficiency in the Hubble Space Telescope Advanced Camera for Surveys," *MNRAS*, vol. 401, pp. 371-384, Jan. 2010.

[3] J. Rhodes, A. Leauthaud, C. Stoughton, R. Massey, K. Dawson, W. Kolbe and N. Roe, "The effects of charge transfer inefficiency (CTI) on galaxy shape measurements," *Publ. Astron. Soc. Pac.*, vol. 122, no. 890, pp. 439-450, Apr. 2010.

[4] J. Gow; N. Murray; A. Holland and D. Burt, "Proton damage comparison of an e2v technologies n-channel and p-channel CCD204," *IEEE Transactions on Nuclear Science* **61(4)** pp.18431848, 2014.

[5] N. Mostek, C. Bebek, A. Karcher, W. Kolbe, N. Roe and J. Thacker, "Charge trap identification for proton-irradiated p+ channel CCDs", *Proc. SPIE*, vol. 7742, pp. 774216, Jul. 2010.

[6] W. Shockley and W. Read Jr., "Statistics of the recombinations of holes and electrons," *Phys. Rev.*, **87(5)**, pp. 835-842, 1952.

[7] R. Hall, "Electron-hole recombination in germanium," *Phys. Rev.*, **87(5)** pp. 387, 1952.

[8] D. Hall, N. Murray A. Holland, J. Gow, A. Clarke and D.Burt, "Determination of in situ trap properties in CCDs using a single trap pumping technique," *IEEE Transactions on Nuclear Science* **61(4)**, 2014.

[9] N. Murray, A. Holland, J. Gow, D. Hall, J. Tutt, D. Burt and J. Endicott, "Mitigating radiation-induced charge transfer inefficiency in full-frame CCD applications by 'pumping' traps," *Proc. SPIE*, vol. 8453, pp. 845317, 2012.

[10] D. Lang, "Deep-level transient spectroscopy: A new method to characterize traps in semiconductors," *J. Appl. Phys.*, **45(7)** pp. 3023-3032, 1974.

[11] J. Gow, D. Wood, D. Burt, D. Hall, B. Dryer, A. Holland and N. Murray, "Initial results from a cryogenic proton irradiation of a p-channel CCD," *SPIE Proceedings*, 2015.

[12] N. Bush; D. Hall; A. Holland; R. Burgeon; N. Murray; J. Gow; M. Soman; D. Jordan; R.T Demers; L.K. Harding; M. Hoenk; D. Michaels; B. Nemati and P.Peddada, "The impact of radiation damage on photon counting with an EMCCD for the WFIRST-AFTA coronagraph," *SPIE Proceedings* 9605, article no. 96050E, 2015.

[13] L.K. Harding; R.T. Demers; M. Hoenk; P. Peddada; B. Nemati; M. Cherng; D. Michaels; L.S. Neat; A. Loc; N. Bush; D. Hall; N. Murray; J. Gow; R. Burgeon; A. Holland; A. Reinheimer; P.R Jorden and D. Jordan, "Technology advancement of the CCD201-20 EMCCD for the WFIRST coronagraph instrument: sensor characterization and radiation damage," *Journal of Astronomical Telescopes, Instruments, and Systems* **2(1)**, 2015.

[14] L.K. Harding; R.T. Demers; M. Hoenk; P. Peddada; B. Nemati; M. Cherng; D. Michaels; A. Loc; N. Bush; D. Hall; N. Murray; J. Gow; R. Burgeon; A. Holland; A. Reinheimer; P.R Jorden and D. Jordan, "Electron multiplication CCD detector technology advancement for the WFIRST-AFTA coronagraph," *SPIE Proceedings*, article no. 96050F, 2015.